Simplicio, P., & Bennani, S. (2015). Worst-case Launch Vehicle Stage Separation Analysis. Paper presented at 3rd CEAS Specialist Conference on Guidance, Navigation and Control, Toulouse, France.

Peer reviewed version

Proceedings of the 3rd CEAS EuroGNC, Specialist Conference on Guidance, Navigation & Control
Co-organized by ONERA, ISAE-SUPAERO & ENAC
Toulouse, France - April 13-15, 2015

Worst-case Launch Vehicle Stage Separation Analysis

P. Simplício and S. Bennani

Abstract This paper is dedicated to the development of a multi-body separation model and to its combination with worst-case simulation methods towards an integrated tool for the verification and validation of launch vehicle stage separation mechanics. The simulator is implemented using SimMechanics, MathWorks' physical modelling suite, and based on the Constraint Force Equation (CFE) framework, which has been previously applied to stage separation simulations. Worst-case problems targeting the analysis of different system requirements (e.g., angular deviation rate or relative translational velocity) are then formulated and applied to the release of a generic payload model as a case-study. Given the outcomes of this study, it is expectable that the worst-case stage separation simulator is able to be directly integrated with different vehicle models, potentially featuring a higher number of dispersed properties, as well as with end-to-end launch vehicle trajectory simulation tools.

1 Introduction and Background

This work aims at illustrating a rapid prototyping cycle for the modelling and assessment of a stage separation system for VEGA launcher payloads. Here, we are interested in the dynamics of multiple vehicles during the separation phase. The modelling approach for the compound between launch vehicle, payload adaptor with separation mechanisms and the payload itself is modelled using the Constrained Force Equation (CFE) formulation, as described in the work of Pamadi and coworkers [8, 5, 6].

Pedro Simplício
ESA ESTEC, Noordwijk 2200, The Netherlands, e-mail: pedro.simplicio@esa.int

Samir Bennani
ESA ESTEC, Noordwijk 2200, The Netherlands, e-mail: samir.bennani@esa.int

A novel physical modelling implementation of the CFE concept applied on generic upper stage separation systems was provided by [1] using Modelica. Inspired by this work and although it is not yet possible to fully exploit MathWorks coding features to generate new types of connectors, a further specialised implementation of the CFE technique including its numerical stabilisation is now realised using the SimMechanics suite. This model is developed to be able to assess dynamic stage separation performance requirements in the face of physical uncertainties in the payload dynamics and separation mechanisms.

In this work, we also aim at showing an alternative assessment strategy to the traditional Monte Carlo analyses, taking advantage of MathWorks design optimisation tools in combination with the SimMechanics separation model developed. Through the available graphical interface, it is straightforward to set parameter ranges that define the referred uncertainty levels. The objective criteria are then set on the signals of interest and the associated optimisation code is executed in order to guide the simulation into its worst-case performance directions. Worst-case simulations objective criteria using various signal L-norm indicators have been tested inspired on the WCSIM tool [7] developed by Seiler et al.

The organisation of the paper is as follows: Sect. 2 shows the implementation of launch vehicle dynamics using SimMechanics, Sect. 3 elaborates on the multi-body dynamics of the two-body system, Sect. 4 introduces the adopted VEGA case-study and Sect. 5 describes the worst-case simulation strategy applied, with which the results obtained are presented in Sect. 6. This work is then concluded with the most relevant remarks in Sect. 7.

2 Launch Vehicle Dynamics in SimMechanics

The first step towards the modelling of stage separation mechanics consists in the implementation of the dynamics of the first body, in this case, the launch vehicle (LV). Using SimMechanics, this is easily achieved with the block diagram depicted in Fig. 1.

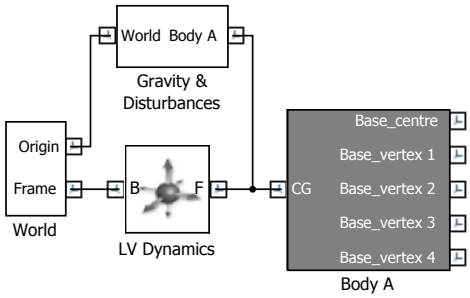

Fig. 1 LV Dynamics schematic

The main advantage of using SimMechanics is that, being a physical modelling tool, every degree-of-freedom (DOF) is introduced via an abstraction to joints and frame transforms, from which the underlying ordinary differential equations (ODEs) are self-generated. In addition, this software has the possibility to make quick changes in model configuration and instrumentation, it provides a direct visualisation of bodies and motions and it is able to be integrated with additional multi-physics packages such as SimElectronics, SimHydraulics or SimPower. For further information on SimMechanics functions or modelling principles the reader is referred to the dedicated documentation from MathWorks [9].

The *LV Dynamics* joint simulates the 6-DOFs motion of body A w.r.t. the inertial world reference frame. This block allows also to specify the initial (orbital) velocity, angular rate and attitude of the LV. In addition, the world reference frame and SimMechanics solver configurations are defined within the *World* subsystem, together with a rigid transform to a local reference frame fixed in the initial position of the body. External force and torque disturbances and gravitational field (modelled as an inverse square force w.r.t. the central body) are also included through the *Gravity & Disturbances* subsystem. The two subsystems referred in this paragraph are illustrated in Fig. 2.

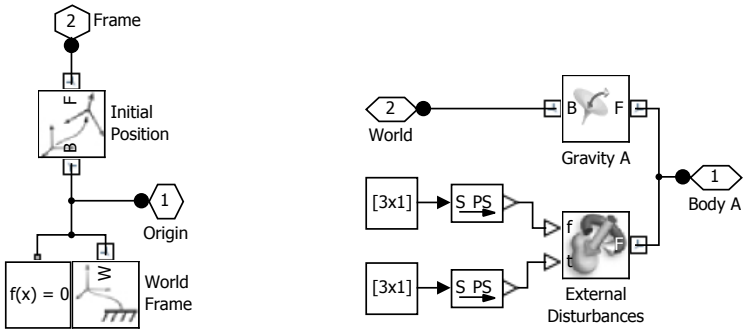

Fig. 2 *World* (*on the left*) and *Gravity & Disturbances* (*on the right*) subsystems

Regarding the LV body (Fig. 3), it is modelled through the SimMechanics *Solid* block, plus a series of rigid transforms to define the orientation of the solid and a set of auxiliary reference frames, e.g., at its centre of gravity (CG). The *Solid* block allows to specify its mass and geometry (either using simple shapes or via an external configuration file), which can be used for the automatic computation of inertial properties (although these can also be provided manually).

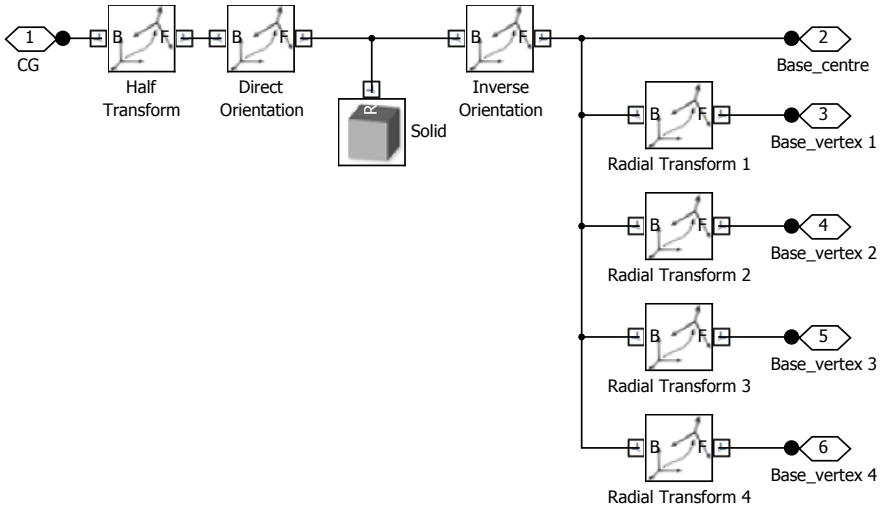

Fig. 3 *Body A* subsystem

3 Joint Constraints and Separation Mechanics

The attachment and relative dynamics between the first and a second body (body B) are also governed by a 6-DOFs SimMechanics joint, as depicted in Fig. 4. Nevertheless, this joint has now actuation and sensing capabilities, which enable the activation of two distinct behaviours:

1. Implementation of motion constraints (*Joint Constraints*) before the separation of the bodies;
2. Removal of those constraints and introduction of the separation impulse (from a *Spring Model*) between bodies once a stage separation trigger signal is commanded.

The joint constraints imposed in this model are based on the Constraint Force Equation (CFE) methodology derived in [11] and applied to stage separation modelling in [8, 5, 6].

Within the referred methodology, three orthogonal relative translation constraints are applied such that the distance between two points remains fixed:

$$(\mathbf{x}_B - \mathbf{x}_A) \cdot \mathbf{e}_A = 0 \tag{1}$$

where $\mathbf{x}_A$ and $\mathbf{x}_B$ are the inertial coordinates of the two points and $\mathbf{e}_A$ represents a unit vector fixed in body A. In addition, three relative rotation constraints are applied such that three combinations of unit vectors $\mathbf{e}_A$ and $\mathbf{e}_B$ remain perpendicular:

$$\mathbf{e}_A \cdot \mathbf{e}_B = 0 \tag{2}$$

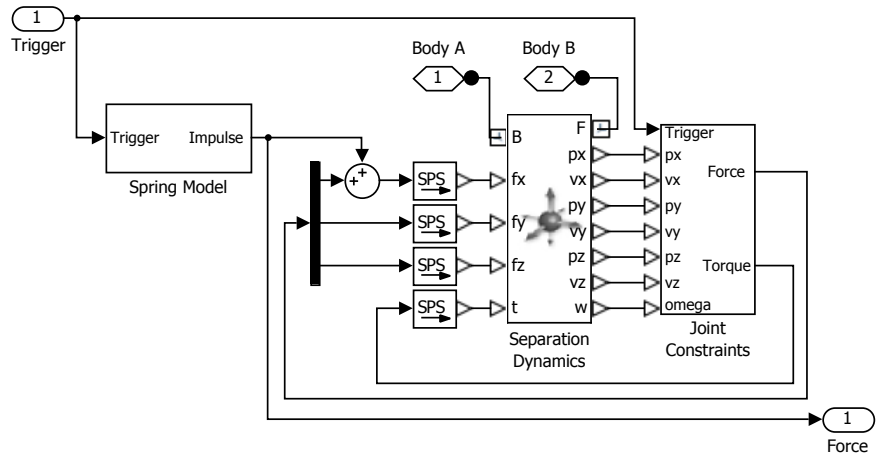

Fig. 4 *Attachment* subsystem

These unit vectors should be normal to the axis about which the unconstrained rotation would take place [11].

The CFE constraints featuring numerical stabilisation have been previously implemented for multi-body simulation using Modelica libraries in [1] and the current paper presents an adaptation of these constraints to SimMechanics, in which custom interfaces cannot be directly linked with its specific 3D multi-body coordinate connectors.

In this case, the 6-DOFs during joint motion are constrained by exerting a force and torque:

$$\mathbf{F}_J = -K_F \Delta \mathbf{x}_J - D_F \Delta \dot{\mathbf{x}}_J \tag{3}$$

$$\mathbf{T}_J = -K_T \Delta \int \omega_J - D_T \Delta \omega_J \approx -K_T \Delta \theta_J - D_T \Delta \dot{\theta}_J \tag{4}$$

where the time dependence was dropped for the sake of simplification and $\Delta \mathbf{x}_J$, $\Delta \omega_J$ and $\Delta \theta_J$ account for joint deviation in terms of position, angular rate and orientation, respectively. The non-negative parameters K_F, D_F, K_T and D_T are tunable and represent a trade-off between modelling accuracy and simulation stiffness.

As mentioned above, once a stage separation trigger signal is commanded, the joint constraints are removed ($\mathbf{F}_J = \mathbf{T}_J = \mathbf{0}$) and the separation impulse is introduced into the system. This is generated by a compressed spring or spring-damper system, aligned with the x-axis of body A ($\mathbf{e}_{x_A}$) and released upon separation ($t = t_{\text{trig}}$). In this paper, a linear undamped spring system is assumed, thus the impulse force is modelled as:

$$\mathbf{F}_S^A(t) = F_{\max} \cos\left[\sqrt{\frac{F_{\max}}{m_S \Delta L}}\left(t - t_{\text{trig}}\right)\right] \mathbf{e}_{x_A}, \tag{5}$$
$$t - t_{\text{trig}} \in \left[0, \frac{\pi}{2}\sqrt{\frac{m_S \Delta L}{F_{\max}}}\right]$$

in which $F_{\max}$ is the maximum spring force, ΔL is the stroke and m_S its equivalent design mass, which is a function of the total energy stored in the separation mechanism.

By putting together the simulation building blocks presented so far, a complete stage separation simulator can be assembled as depicted in Fig. 5. In this case, the multi-body system is initially connected through four identical *Attachment* subsystems (Fig. 4), applied in different points and which may be triggered simultaneously or at distinct time instants.

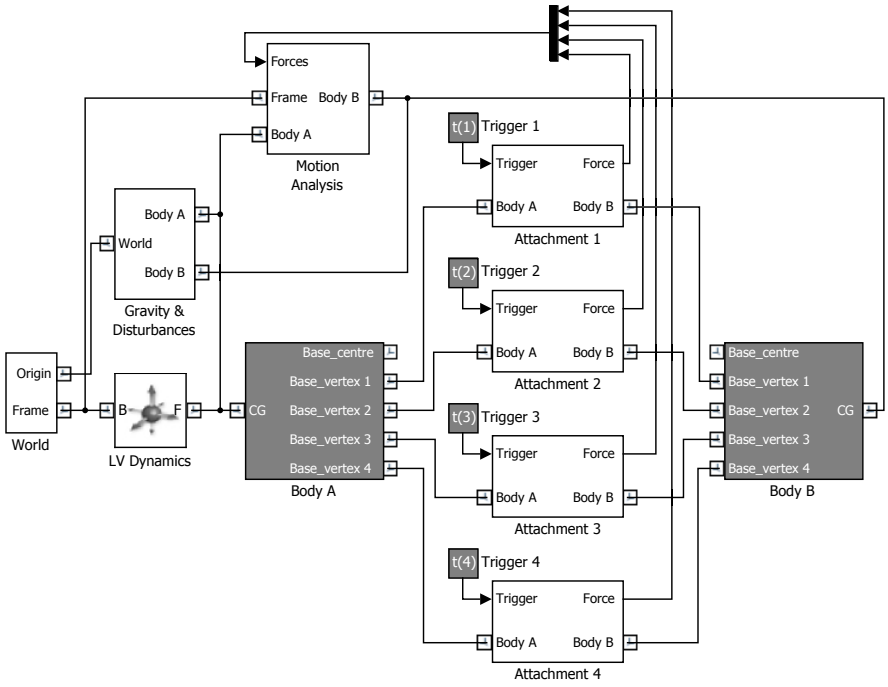

Fig. 5 Multi-spring stage separation simulator

Furthermore, Fig. 5 features a *Motion Analysis* subsystem that comprises SimMechanics transform sensors and scopes to quantify the translational and rotational motion of body B relative to the initial LV trajectory and to body A. In addition, this subsystem computes the linear and angular momentum transmitted to body B

as a result of the spring impulses. These linear and angular momentum changes are given by:

$$\Delta \mathbf{p}_B(t) = \int_0^t \sum_{i=1}^{4} \mathbf{F}_{S_i}^B(\tau)\,\mathrm{d}\tau \tag{6}$$

$$\Delta \mathbf{L}_B(t) = \int_0^t \sum_{i=1}^{4} \left(\mathbf{x}_i^B - \mathbf{x}_{CG}^B\right) \times \mathbf{F}_{S_i}^B(\tau)\,\mathrm{d}\tau \tag{7}$$

where $\mathbf{x}_{CG}^B$ are the local coordinates of the CG of body B and $\mathbf{x}_i^B$ are the coordinates of the i-th attachment point. In addition, $\mathbf{F}_{S_i}^B(t)$ is the impulse force transmitted by spring i written in body B reference frame, which is determined from:

$$\mathbf{F}_{S_i}^B(t) = [\mathbf{C}_{\mathbf{q}_{A\to B}}(t)]\,\mathbf{F}_{S_i}^A(t) \tag{8}$$

in which $\mathbf{F}_{S_i}^A(t)$ is given by Eq. 5 for each spring and $[\mathbf{C}_{\mathbf{q}_{A\to B}}(t)]$ is the direction cosine matrix [4] built from the quaternions that represent the rotation between the two bodies (measured within the subsystem).

4 VEGA Case-study

This section introduces the application of the multi-spring stage separation simulator to the analysis of VEGA payload separation. The separation between the two bodies is a very critical phase of a mission, thus strict requirements are set in order to avoid the possibility of a subsequent collision between the payload and the LV upper module, as exemplified in Table 1.

Table 1 Separation requirements

Conditions after separation	Requirement (3σ)
Angular rate modulus (deg/s)	$\leq$ [1.5 1.5 1.5]
Angular deviation (deg)	$\leq$ [1.5 1.0 1.0]
Long. speed w.r.t. LV (m/s)	≥ 0.5

The main objective of this study is therefore to provide the means to verify if the requirements of Table 1 are fulfilled, taking into account that system properties are defined with certain tolerance levels around their nominal values (Table 2), as well as the worst-case attitude specifications of VEGA's upper stage just before separation (Table 3).

In order to tackle this problem and accomplish the objective mentioned above, a worst-case simulation analysis approach is selected and applied to the separation model, as further described in the following section.

Table 2 Dispersed properties of the case-study

System property	Nominal	Tolerance
Mass (kg)	1860	±20
CG Location (mm)	[1933 1 8]	[±20 ±13 ±13]
Inertia moments (kg.m^2)	[669 3136 3265]	[±70 ±320 ±330]
Inertia products (kg.m^2)	[0 0 0]	[±130 ±130 ±130]
Maximum spring forces (N)	1485.[1 1 1 1]	[±15 ±15 ±15 ±15]
Spring strokes (mm)	121.[1 1 1 1]	[±1.2 ±1.2 ±1.2 ±1.2]

Table 3 Worst-case LV attitude specifications before separation

LV Attitude before separation	Specification
Angular rate (deg/s)	[0.576 0.327 0.327]
Angular deviation (deg)	[0.466 0.479 0.461]

5 Worst-case Simulation

Consider the nonlinear system generically represented as:

$$\begin{aligned} \dot{\mathbf{x}}(t) &= \mathbf{f}(\mathbf{x}(t), \mathbf{p}, t) \\ \mathbf{y}(t) &= \mathbf{h}(\mathbf{x}(t), \mathbf{p}, t) \\ \mathbf{x}(0) &= \mathbf{x}_0 \end{aligned} \tag{9}$$

in which $\mathbf{x}(t) \in \mathbb{R}^{n_x}$ is the state at time t, $\mathbf{y}(t) \in \mathbb{R}^{n_y}$ is the output, $\mathbf{x}_0 \in \mathbb{R}^{n_x}$ is the initial state, $\mathbf{p} \in \mathscr{P} \subseteq \mathbb{R}^{n_p}$ is a constant parameter vector from the allowable subset of values $\mathscr{P}$ upon which the model depends and $\mathbf{f}$, $\mathbf{h}$ are vector fields.

Worst-case simulation is a robustness analysis performed directly on such a system to study the influence of the dispersed model properties $\mathscr{P}$ on the variation of the output $\mathbf{y}(t)$ [7]. More precisely, worst-case simulation aims to find combinations of properties that yield high output degradations (deviations from the nominal response), which is formalised as the following optimisation problem:

$$\begin{aligned} \max_{\mathbf{p} \in \mathscr{P}} \quad & G(\mathbf{y}(t)) \\ \text{s.t.} \quad & \text{Eq. 9} \end{aligned} \tag{10}$$

This problem can be solved using a variety of algorithms [3] and tools such as the WCSIM presented in [7]. Further constraints may be introduced if necessary and the objective function $G(\mathbf{y}(t))$ should represent a scalar measure of the output degradation (i.e., anti-optimisation).

The method applied in this study relies on Simulink's Response Optimization tool (part of its Design Optimization toolbox) as it offers a straightforward graphical interface with the SimMechanics system and its variables. Further documentation

on this toolbox can be found in [10]. The selected algorithm uses a gradient-based sequential quadratic programming (SQP) solver for the optimisation problem. As it is generally not a concave problem, this algorithm may not find a global maximum, but provides an assessment of critical parameter vectors.

The worst-case stage separation algorithm is initialised with the nominal parameters $\mathbf{p}$ of Table 2 and initial conditions $\mathbf{x}_0$ of Table 3. At each iteration, the solver evaluates the objective function at current parameter values and at small perturbations along each direction, performing a total of $n_p + 1 = 19$ simulations per iteration.

Furthermore, the objective function shall render the output degradation in terms of the requirements listed in Table 1. In this sense, worst-case conditions are those at which the angular rate of the payload after separation (or alternatively the angular momentum change from Eq. 7) is maximised and at which its longitudinal speed (or alternatively the linear momentum change from Eq. 6) is minimised. To account with these, different signal L-norm indicators [2] are employed as objective functions:

$$G_{L_1} = L_1(\omega(t)) = \int_0^t \sum_{i=1}^{3} |\omega_i(\tau)| \, \mathrm{d}\tau \tag{11}$$

$$G_{L_2} = L_2(\omega(t)) = \sqrt{\int_0^t \sum_{i=1}^{3} \omega_i^2(\tau) \, \mathrm{d}\tau} \tag{12}$$

$$G_{L_\infty} = L_\infty(\omega(t)) = \sum_{i=1}^{3} \max |\omega_i(t)| \tag{13}$$

$$G_{PM} = -\max v_x(t) \tag{14}$$

where $\omega(t)$ and $v_x(t)$ are respectively the angular rate and longitudinal speed of the payload relative to the LV. The results obtained with this worst-case simulation methodology are summarised in the next section.

6 Simulation Results

This section presents the main results obtained with the application of the worst-case simulation described in Sec. 5 to the stage separation model introduced in Sec. 4. The translational and rotational motion of the payload over the first three seconds after separation is registered in Figs. 6 and 7, respectively. These figures depict the response of the nominal system (marked with $*$), as well as the degraded responses found with the four worst-case objective functions proposed.

Starting with the nominal case to get the perception of the underlying physical phenomena, it is possible to observe the linear acceleration and consequent momentum changes introduced by the separation impulses in the longitudinal (x) axis of the payload (second and third plots of Fig. 6). These changes are reflected into the

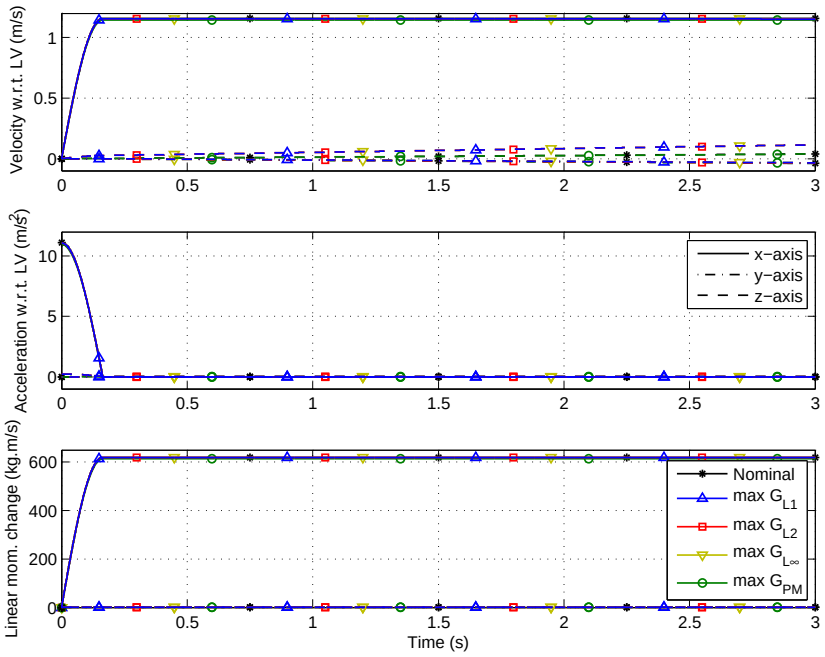

Fig. 6 Translational analysis of the separation dynamics

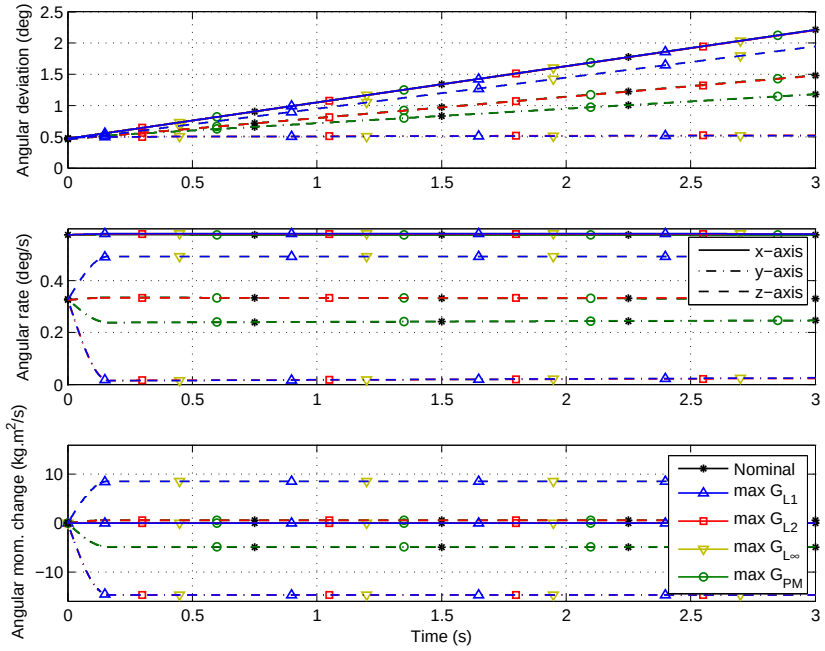

Fig. 7 Rotational analysis of the separation dynamics

increase of velocity relative to the LV (first plot of Fig. 6). Very small changes are also transmitted in the lateral (y) and vertical (z) directions due to Eq. 8 once the two bodies are separated and due to the gravity gradient between them. In addition, angular momentum changes are introduced in the system according to Eq. 7 because of the displacement between payload CG and the attachment points (third plot of Fig. 7). This effect is then propagated into the increase of angular deviations and rates, which are already non-zero before separation (first and second plots of Fig. 7).

The most representative characteristics of the degraded responses showed in the plots are described below and compiled into Table 4, which provides a comparison with the data of Tables 1 and 2.

Table 4 Comparison of worst-case results (M=maximum, m=minimum, Nom=nominal)

Conditions after separation	Requirement	max G_{L_1},G_{L_∞}	max G_{L_2}	max G_{PM}
Angular rate modulus (deg/s)	$\leq$ [1.5 1.5 1.5]	[0.58 0.02 0.49]	[0.58 0.02 0.33]	[0.58 0.24 0.33]
Angular deviation[a] (deg)	$\leq$ [1.5 1.0 1.0]	up to $t = 1.1$ s	up to $t = 1.6$ s	up to $t = 1.6$ s
Long. speed w.r.t. LV (m/s)	$\geq$ 0.5	1.16	1.16	1.14
System property	**Nominal**	**max G_{L_1},G_{L_∞}**	**max G_{L_2}**	**max G_{PM}**
Mass (kg)	1860	M	M	M
CG Location (mm)	[1933 1 8]	[M M M]	[M Nom M]	$\approx$Nom
Inertia moments (kg.m^2)	[669 3136 3265]	[M m m]	[$\approx$M m m]	$\approx$Nom
Inertia products (kg.m^2)	[0 0 0]	$\approx$Nom	$\approx$Nom	$\approx$Nom
Maximum spring forces (N)	1485.[1 1 1 1]	[m m M M]	[m m M M]	[m m m m]
Spring strokes (mm)	121.[1 1 1 1]	[m m M M]	[m m M M]	[m m m m]
Number of solver iterations	–	8	5	2

[a] Angular deviation requirements are assessed in terms of the time up to which they are fulfilled since these angles increase at an approximately constant rate.

The worst-case problem characterised by function G_{PM} (from Eq. 14, marked with $\circ$ in the plots) is the one that yields the least response degradation. In fact, only the translational motion is affected. As represented in the table, the solver finds this solution simply by setting the payload mass to its maximum allowable value and all the spring forces and strokes to their minimum, so that the transmission of linear momentum between bodies is minimised. Only two iterations were required by the solver to converge into this solution.

A more intense degradation is then achieved with G_{L_2} (from Eq. 12, marked with $\square$ in the plots), especially in terms of rotational motion. The worst-case solution found with this objective function corresponds to the angular momentum maximisation around only one of the body axes (y-axis in this case, as depicted in Fig. 7). As indicated in the table, this is mainly achieved by 1) minimising the payload lateral inertia moments while maximising its longitudinal inertia and CG shift along the z-axis and 2) setting symmetric force and stroke capabilities to the springs above and under the body xy-plane. As a result of the more intense rotation, part of the linear momentum transmitted during separation is lost from the longitu-

dinal axis to the other ones (Fig. 6). The computation of this solution required three more iterations than the previous one, being therefore slightly more demanding.

Finally, objective functions G_{L_1} (from Eq. 11, marked with $\triangle$ in the plots) and G_{L_∞} (from Eq. 13, marked with $\triangledown$), which converged into the same worst-case solution, allow to extend the degradation generated with G_{L_2} to all the payload axes, thus maximising all the angular momentum components. Comparing to the previous solution, this is naturally achieved by setting the CG shifts along the three axes to their maximum allowable values. The consequences for the translational motion are similar to the former case. The resolution of this problem is however more demanding, requiring eight iterations for the solver to converge.

As illustrated in Table 4, VEGA separation requirements are fulfilled for all the conditions analysed in the scope of this study. Nonetheless, the ability of this model to capture the underlying physical phenomena evidences the applicability of the worst-case stage separation simulator to the analysis of a wide range of requirement types and different vehicle models, which may involve allowable parameter sets with higher dimensions.

7 Conclusions and Future Work

The SimMechanics-based model developed within this study represents a simple and modular approach to investigate the dynamics of multi-body separation, as well as the influence of different system properties and initial conditions in this motion. The relative constraints and mechanics implemented are inclusively well suited to be integrated with end-to-end launch vehicle trajectory simulation tools and generate stage separation analyses with an increased level of detail.

Furthermore, the proposed interface with Simulink's Response Optimization toolbox enables the direct formulation and resolution of different worst-case problems, as showed in the paper, targeting the analysis of different system requirements (e.g., angular deviation rate or relative translational velocity). This approach is particularly useful to the verification and validation of complex systems such as the separation mechanisms responsible for the successful release of a payload into space.

As a short-term development of the work that has been carried out, the worst-case stage separation simulator will be further augmented with a dedicated clearance analysis between critical elements of the payload, such as antennas or solar panels. This will then provide a thorough insight on worst-case collision risks and safety margins after separation.

Acknowledgements The authors would like to acknowledge the recommendations and technical assistance provided by A. Rinalducci, X. Lefort, C. Roux and the VEGA Integrated Project Support Team. This work has been carried out under a traineeship grant supported by the Portuguese Foundation for Science and Technology (FCT).

References

1. Acquatella B., P. and Reiner, M.J. (2014) Modelica Stage Separation Dynamics Modeling for End-to-End Launch Vehicle Trajectory Simulations. In the 10th International Modelica Conference, March 10-12 2014, Lund, Sweden.
2. Doyle, J., Francis, B. and Tannenbaum, A. (1990) Feedback Control Theory. Macmillan Publishing Co.
3. Gill, P.E., Murray, W. and Wright, M.H. (1981) Practical Optimization. Academic Press, Inc.
4. Kuipers, J.B. (2002) Quaternions and Rotation Sequences. Princeton University Press.
5. Pamadi, B.N., Pei, J., Pinier, J.T., Holland, S.D., Covell, P.F. and Klopfer, G.H. (2012) Aerodynamic Analyses and Database Development for Ares I Vehicle First-stage Separation. Journal of Spacecraft and Rockets, Vol. 49, No. 5, pp. 864-874.
6. Pamadi, B.N., Tartabini, P.V., Toniolo, M.D., Roithmayr, C.M., Karlgaard, C.D. and Samareh, J.A. (2013) Application of Constraint Force Equation Methodology for Launch Vehicle Stage Separation. Journal of Spacecraft and Rockets, Vol. 50, No. 1, pp. 191-205.
7. Seiler, P., Balas, G. and Packard, A. (2012) Worst-case Simulation with the GTM Design Model. In ESA-CNES-DLR Workshop on Worst Case Analysis Tools for Guidance Navigation & Control Systems, November 13-14 2012, ESA ESTEC, The Netherlands.
8. Tartabini, P.V., Roithmayr, C.M., Toniolo, M.D., Karlgaard, C.D. and Pamadi, B.N. (2011) Modeling Multibody Stage Separation Dynamics using Constraint Force Equation Methodology. Journal of Spacecraft and Rockets, Vol. 48, No. 4, pp. 573-583.
9. The MathWorks, Inc. (2014) SimMechanics Documentation. http://www.mathworks.nl/help/physmod/sm/index.html, accessed Oct. 2014.
10. The MathWorks, Inc. (2014) Simulink Response Optimization Documentation. http://www.mathworks.nl/help/sldo/index.html#response-optimization, accessed Oct. 2014.
11. Toniolo, M.D., Tartabini, P.V., Pamadi, B.N. and Hotchko, N. (2008) Constraint Force Equation Methodology for Modeling Multi-body Stage Separation Dynamics. In the 46th AIAA Aerospace Sciences Meeting and Exhibit, January 7-10 2008, Reno, Nevada.